CCSD(T) study of the far-infrared spectrum of ethyl methyl ether

M. L. Senent,[1,a)] R. Ruiz,[2] M. Villa,[3] and R. Domínguez-Gómez[4]
[1]*Departamento de Astrofísica Molecular e Infrarroja, Instituto de Estructura de la Materia, CSIC, Serrano 121, Madrid 28006, Spain*
[2]*Departamento de Química, Universidad de Burgos, Plaza Misael Bañuelos s/n, 09001 Burgos, Spain*
[3]*Departamento de Química, UAM-I Purísima y Michoacan, s/n, CP 09340 Mexico, Distrito Federal, Mexico*
[4]*Departamento de Ingeniería Civil, Cátedra de Química, EUIT Obras Públicas, Universidad Politécnica de Madrid, Madrid 28014, Spain*

(Received 16 September 2008; accepted 5 January 2009; published online 9 February 2009)

Band positions and intensities for the far-infrared bands of ethyl methyl ether are variationally determined from a three-dimensional (3D) potential energy surface calculated with CCSD(T)/cc-pVTZ theory. For this purpose, the energies of 181 selected geometries computed optimizing $3n-9$ parameters are fitted to a 3D Fourier series depending on three torsional coordinates. The *zero point vibrational energy* correction and *the search of a correct definition of the methyl torsional coordinate* are taken into consideration for obtaining very accurate frequencies. In addition, second order perturbation theory is applied on the two molecular conformers, *trans* and *cis-gauche*, in order to test the validity of the 3D model. Consequently, a new assignment of previous experimental bands, congruent with the new *ab initio* results, is proposed. For the most stable *trans*-conformer, the ν_{30}, ν_{29}, and ν_{28} fundamental transitions, computed at 115.3, 206.5, and 255.2 cm^{-1}, are correlated with the observed bands at 115.4, 202, and 248 cm^{-1}. For the *cis-gauche* the three band positions are computed at 91.0, 192.5, and 243.8 cm^{-1}. Calculations on the $-d_3$ isotopomer confirm our assignment. Intensities are determined at room temperature and at 10 K. Structural parameters, potential energy barriers, anharmonic frequencies for the $3n-9$ neglected modes, and rotational parameters (rotational and centrifugal distortion constants), are also provided. © *2009 American Institute of Physics*. [DOI: 10.1063/1.3073895]

I. INTRODUCTION

The correlation between abundance of ethers and alcohols in astrophysical sources has been frequently pointed out, as both compound types are involved in common chemical processes. Thus, it appears reasonable to presuppose the existence of ethyl methyl ether (EME) in objects where ethanol abundance is significant, in the same way as dimethyl ether and methanol usually coexist.[1,2]

Recently, EME has been tentatively proposed as responsible of some rotational spectral lines observed in hot cores associated with regions of high-mass star formation, where the abundance of ethers such as dimethyl ether, is evident.[1] Before this uncertain detection, EME attracted low attention even though the relevance for radioastronomy and the miss at point of the new instruments for detection, as ALMA, have motivated laboratory measures of rotational spectra of many ethers.[3–13] Currently, Fuchs *et al.*[3] recorded the spectrum for the vibrational-torsional ground state assigning and making predictions of line positions up to 450 GHz, extending the previous assigned frequency intervals of Hayashi and Kuwada,[4] Hayashi and Adachi,[5] and Tsunekawa *et al.*[6] Kobayashi *et al.*[7] recorded and analyzed the microwave spectrum in the first skeletal torsionally excited state.

It may be expected that the new radioastronomical instruments will be capable of receiving new signals corresponding to simplest organic compounds favoring their characterization and demanding detailed astrophysical catalogs for their understanding. The observation assignments will require knowledge of the rovibrational spectrum at low temperature at which the first vibrational levels can be populated. However, the complex spectroscopic properties of EME, which display various large amplitude vibrations, make the interpretation of experimental data difficult. For example, three low frequency modes, which intertransform 27 minima separated by feasible barriers, confer nonrigid properties to the molecule. The three vibrations are the $O-C_2H_5$ torsion (ν_{30}), the $O-CH_3$ torsion (ν_{29}), and the $C-CH_3$ torsion (ν_{28}). On the base of state-of-the art *ab initio* calculations, we look at the assignments of Durig *et al.*[14] These authors recorded the Raman and infrared spectra for the gas phase (between 35 and 350 cm^{-1}) and in annealed solids, giving a large amount of information related to the spectroscopy of the molecule.

It is commonly accepted that *ab initio* calculations can help experimental research if the level of the theory is high enough, as occurs with the size-consistent couple cluster theory [CCSD(T)] applied to monoconfigurational systems.[15] For nonrigid molecules, the theory can help in understanding many aspects related to the effects of barriers on the splitting of the levels.[16–18] To take all these effects into consideration, the torsional spectrum of EME is studied, in this paper, from a CCSD(T) three-dimensional potential energy surface (3D-PES) and a flexible variational model. The 3D-PES determi-

a)Author to whom correspondence should be addressed. Electronic mail: senent@damir.iem.csic.es.

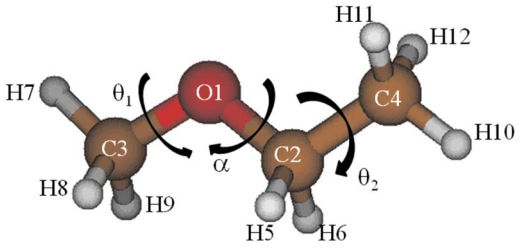

FIG. 1. (Color online) The minimum energy structure of *trans*-ethyl methyl ether and the three torsional coordinates.

nation (12 atoms; 181 optimized geometries + zero vibrational energy correction) has carried out a large computational effort. We would like to remark that the few previous theoretical studies of EME have been performed at lower levels of theory dealing with a reduced number of geometries. Furthermore, simpler one-dimensional model (for ethyl group torsion)[14] or two-dimensional models (for the two methyl groups)[3,19] were employed. In the current work, we include interactions among the three internal rotations.

Variational spectroscopic parameters are compared with the available experimental data and with the results obtained in this work using second order perturbation theory (PT2) from *ab initio* anharmonic force fields.[20] The results allow us to propose a new assignment of the far-infrared (FIR) bands measured by Durig *et al.*[14]

II. COMPUTATIONAL DETAILS

The search of the minimum energy geometries has been performed at the CCSD/cc-pVTZ level. The 3D-PES, depending on the three torsional angles, has been determined from the CCSD(T)/cc-pVTZ electronic energies of a grid of 181 selected geometries. For all the structures, $3n-9$ internal coordinates have been optimized at the CCSD/cc-pVTZ level. CCSD/cc-pVTZ harmonic fundamentals and MP2/cc-pVTZ anharmonic fundamentals have been computed using the algorithms implemented in GAUSSIAN 03.[21]

The 3D variational calculation of the torsional band positions and the corresponding band intensities have been calculated with our code ENEDIM[22] developed for the study of acetic acid.[23] All the calculations have been performed in our high performance system GRID and CESGA computational facilities.

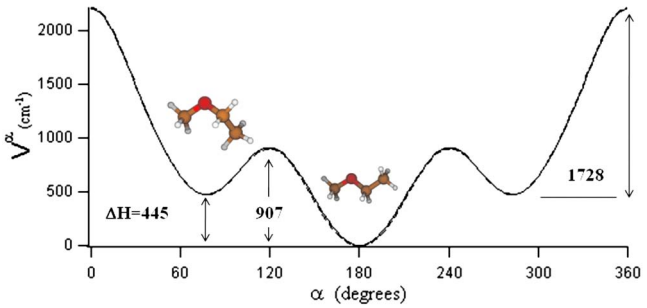

FIG. 2. (Color online) One-dimensional cut of the PES along the torsional coordinate, α.

TABLE I. CCSD/cc-pVTZ structural parameters (distances in Å; angles in deg) and rotational constants (in MHz) corresponding to the two conformers, *trans* [E(CCSD/cc-pVTZ)=−193.991 629 a.u.; E(CCSD(T))/cc-pVTZ=−194.021 508 a.u.] and *cis-gauche* [E(CCSD/cc-pVTZ)=−193.989 447 a.u.; E(CCSD(T))/cc-pVTZ=−194.019 478 a.u.], of ethyl methyl ether.

	trans	*gauche*
C2O1	1.4106	1.4132
C3O1	1.4062	1.4074
C4C2	1.5132	1.5220
H5C2	1.0973	1.0972
H6C2	1.0973	1.0895
H7C3	1.0872	1.0875
H8C3	1.0958	1.0960
H9C3	1.0958	1.0937
H10C4	1.0902	1.0909
H11C4	1.0894	1.0898
H12C4	1.0894	1.0898
C3O1C2	111.6	113.1
C4C2O1	108.6	113.5
H5C2O1	109.9	109.8
H6C2O1	109.9	105.6
H7C3O1	107.6	107.3
H8C3O1	111.4	111.2
H9C3O1	111.4	112.4
H10C4C2	110.4	109.9
H11C4C2	110.4	110.2
H12C4C2	110.4	112.0
C4C2O1C3	180.0	74.1
H5C2O1C4	−121.0	−123.9
H6C2O1C4	121.0	120.3
H7C3O1C2	180.0	173.8
H8C3O1C2	−60.6	54.9
H9C3O1C2	60.6	−67.0
H10C4C2O1	180.0	174.6
H11C4C2O1	−59.9	55.1
H12C4C2O1	59.9	−65.7
A	28 341.5	15 993.7
B	4193.2	5223.6
C	3921.5	4546.3

III. DISCUSSION AND CONCLUSIONS

A. Equilibrium geometries

EME presents three torsional modes which are responsible for the nonrigid properties of the molecule, the O–C_2H_5 torsion (ν_{30}), the O–CH_3 torsion (ν_{29}), and the C–CH_3 torsion (ν_{28}). We call α, θ_1, and θ_2 the three corresponding vibrational coordinates (see Fig. 1). The analytical form of the 3D energy surface may be expressed as a 3D Fourier series,

$$V(\alpha,\theta_1,\theta_2) = \sum_{l=0}\sum_{m=0}\sum_{n=0}[\cos(l\alpha)\cos(3m\theta_1)\cos(3n\theta_2) + \sin(l\alpha)\sin(3m\theta_1)\cos(3n\theta_2) + \sin(l\alpha)\cos(3m\theta_1)\sin(3n\theta_2) + \cos(l\alpha)\sin(3m\theta_1)\sin(3n\theta_2)]. \quad (1)$$

The level of *ab initio* calculations has been selected by

TABLE II. Relative energy between the two conformers (ΔH, in cm^{-1}) and torsional barriers (in cm^{-1}), for ethyl methyl ether [$V_3(O-CH_3)=E(\alpha,180,180)-E(\alpha,0,180)$; $V_3(C-CH_3)=E(\alpha,180,180)-E(\alpha,180,0)$ $V(trans \rightarrow gauche)=E(90,180,180)-E_{trans}$; $V(gauche \rightarrow gauche)=E(180,180,180)-E_{cis\text{-}gauche}$].

	MP2/cc-pVTZ	CCSD(T)/cc-pVTZ	CCSD(T)/cc-pVTZ+ZPVE	Fitted from expt. freq. (Ref. 14)
		trans → *gauche*		
ΔH	478	445	484	550 ± 6
$V^{trans \rightarrow gauche}$	956	907	935	958
$V^{gauche \rightarrow gauche}$	1801	1728	1742	631
α	73°	74°	74°	74.1°
		trans		
V_3 (O–CH_3)	909	871	890	
V_3 (C–CH_3)	1123	1079	1120	
		gauche		
V_3 (O–CH_3)	660	639	637	
V_3 (C–CH_3)	1030	996	1024	

taken into consideration in Ref. 24. The search of the minimum energy geometries has been performed with CCSD/cc-pVTZ calculations. Later on, single point CCSD(T) energies have been computed for each optimized structure. The ethyl group rotation interconverts two different isomers, *trans* and *cis-gauche*, corresponding to 180° and 74.1° values of the C4C2O1C3 dihedral angle, respectively (see Fig. 1). The *trans*-form represents the total minimum and referential geometry, although the enthalpy difference between both minima, ΔH, is only 445 cm^{-1} [CCSD(T)/cc-pVTZ]. Both forms are separated by a relatively low barrier of 445 cm^{-1}. Steric interactions between methyl group hydrogens make the *cis*-structure, which lies 1728 cm^{-1} over the *trans*-form, unstable. Figure 2 displays the variation in the total electronic energy with the ethyl torsion. For each isomer, the internal rotation of the two methyl groups, θ_1 and θ_2, defines nine minima and produces a characteristic egg-box shape for the PES.

Table I shows the structural parameters and the equilibrium rotational constants of the two isomers. To avoid steric interactions, the ethyl group rotation carries out a significant skeletal deformation especially visible for the C4C2O1 planar angle which varies 5° during the rotation (from 108.6° at the *trans*-form to 113.5° at the *gauche*-form). A minor variation in the molecular center of mass and a minor molecular deformation accompany the methyl group torsion. The most important parameters for radioastronomy, the rotational constants, have been calculated to be 28 341.5, 4193.2, and 3921.5 MHz for *trans*-EME and 15 993.7, 5223.6, and 4546.3 MHz for *cis-gauche*-EME. Both structures are near prolates although the antisymmetric character augments in the *cis-gauche*-form.

In Table II, we compare the energy barriers calculated at the CCSD(T)+ZPVE level with the other ones determine in the present work with the Möller–Plesset theory and with those of Durig *et al.*[14] obtained by fitting observed frequencies. These last barriers have been determined using a one-dimensional effective Hamiltonian that averaged many properties. Thus, since the model employed for their determination is not similar to our model, they are not quantitative comparable to our parameters, although they give an idea about the correct order of magnitude. For example, our ΔH (484 cm^{-1}) has been obtained optimizing $3N-6$ coordinates for both conformers, not in one dimension. However, it is evident how the zero point vibrational energy (ZPVE) correction approaches the corresponding value in Ref. 14 because of the collective effects considered in the effective Hamiltonian. In the table, we detailed the definitions employed for the torsional barriers. As is shown in Ref. 24, an enlargement of the cc-pVTZ basis set does not change the torsional barrier significantly (see Fig. 3).

B. Vibrational anharmonic force field

If tunneling splittings are negligible, then the anharmonic analysis based on the FG formalism and PT2 is a good approximation for the determination of vibrational transition connecting levels lying close to the PES minima. For us, it represents a helpful method to provide preliminary information about the vibrational interactions between torsions and vibrations neglected in our 3D model.

TABLE III. Displacements of the torsional levels by vibrational resonances (in cm^{-1}).

Mode		E	ΔE
	trans-EME		
$V29=1$	O–CH_3	457	4
$V28=1$	O–C_2H_5		
	cis-gauche-EME		
$V21=1$	O–CH_3	1321	−2
$V29=1$	CH_3-rock		
$V28=1$	O–CH_3	430	2
$V29=1$	O–C_2H_5		
$V27=1$	CCO bend	477	−1
$V30=1$	O–C_2H_5		

TABLE IV. Harmonic and anharmonic fundamentals (in cm^{-1}) corresponding to the two conformers, *trans* and *cis-gauche*, of ethyl methyl ether, calculated with the cc-pVTZ basis set.

		trans					*gauche*			
N ν_N	Mode	υ (expt)	υ MP2	ω-υ MP2	ω CCSD	Mode	υ (expt)	υ MP2	ω-υ MP2	ω CCSD
19 A''	CH_3-asym. stretch	2995	3046	138	3148	1		3043	138	3146
1 A'	CH_3-asym. stretch	2981	3046	135	3145	2		3042	135	3143
2 A'	CH_3-asym. stretch	2935	3042	137	3141	3		3034	135	3133
20 A''	CH_3-asym. stretch	2906	2957	131	3064	4	2906	3004	132	3107
3 A'	CH_3-sym. stretch	2954	3016	71	3058	5		2974	128	3072
21 A''	CH_2-asym. stretch	2893	2916	135	3029	6		2999	82	3060
4 A'	CH_3-sim. stretch	2869	2944	81	3010	7		2875	156	3017
5 A'	CH_2-sim. stretch	2835	2872	139	2998	8		2894	134	3011
6 A'	CH_2-sym. def.		1506	41	1554	9		1479	55	1539
7 A'	CH_3-asym. def	1464	1465	62	1530	10		1490	37	1532
8 A'	CH_3-asym. def		1483	34	1521	11		1474	39	1519
22 A''	CH_3-asym. def		1503	4	1511	12		1471	36	1513
23 A''	CH_3-asym. def	1456	1472	28	1504	13		1460	40	1505
9 A'	CH_3-sym. def.	1448	1484	3	1499	14		1473	10	1495
10 A'	CH_3-sym. def	1396	1399	35	1452	15		1387	33	1438
11 A'	CH_2-wag	1368	1369	31	1414	16		1364	32	1410
24 A''	CH_2-twist	1277	1280	30	1318	17	1310	1312	35	1358
12 A'	CH_3-rock	1214	1218	29	1265	18		1217	30	1262
25 A''	CH_3-rock	1175	1181	28	1219	19	1114	1179	35	1232
13 A'	COC-asym. stretch.	1135	1147	35	1197	20		1162	28	1199
26 A''	CH_3-rock		1156	22	1186	21		1120	26	1156
14 A'	CH_3-rock	1100	1102	24	1133	22	1072	1080	26	1112
15 A'	C–C-stretch	1020	1030	27	1064	23		995	23	1027
16 A'	COC-sym. stretch.	858	864	17	888	24	845	849	18	875
27 A''	CH_3-rock		823	4	830	25		804	4	812
17 A'	COC-bend		473	−4	474	26		461	4	469
18 A'	CCO-bend	288	289	1	293	27		377	4	385

TABLE V. Fundamental frequencies (in cm^{-1}) for *trans* and *cis-gauche*-EME.

	MP2					CCSD	CCSD(T)			Expt.	
	ω	υ	3D	3D+ZPVE	3D+ZPVE+DihC	ω	3D	3D+ZPVE	3D+ZPVE+DihC	new (old)	Δ^a
					trans-EME						
ν_{28} $C-CH_3$ torsion	265	259	246.3	251.0	261.4	262	240.8	245.7	255.2	248 (278)	7.2
ν_{29} $O-CH_3$ torsion	215	211	197.1	200.8	211.3	212	192.8	196.6	206.5	202 (248)	4.5
ν_{30} $O-C_2H_5$ torsion	116	118	114.5	118.0	118.1	114	111.9	115.4	115.3	115.4 (115.4)	−0.1
					cis-gauche-EME						
ν_{28} $C-CH_3$ torsion	267	242	242.1	246.1	250.9	260	236.8	240.6	243.8		
			242.1	246.1	250.9		236.8	240.6	243.8		
ν_{29} $O-CH_3$ torsion	204	198	192.2	191.1	195.6	201	189.7	193.1	192.5		
			192.2	191.1	195.6		189.7	193.1	192.5	(202)	
ν_{30} $O-C_2H_5$ torsion	86	95	92.8	92.5	93.1	82	91.7	91.0	91.0	93.56 (93.56)	−2.6
			92.8	92.5	93.1		91.7	91.0	91.0		

trans-$CD_3-O-CH_2-CH_3$

	ν_{28} $C-CH_3$ torsion	ν_{29} $O-CH_3$ torsion	ν_{30} $O-C_2H_5$ torsion
3D+ZPVE+DihC	249.0	166.6	106.2
Expt. (Ref. 14) old=new	241	163	106
Δ^a	8.0	3.6	0.2

[a]Δ=(3D+ZPVE+DihC)–Expt. (Ref. 14) (new assignment).

TABLE VI. Torsional energy levels corresponding to the nondegenerate representation A_1 and A_2, calculated with CCSD(T)/cc-pVTZ.

trans-EME						*cis-gauche*-EME		
$vv'v''$	Symmetry	E (cm^{-1})	$vv'v''$	Symmetry	E (cm^{-1})	$vv'v''$	Symmetry	E (cm^{-1})
000	A_1	0.00[a]	310	A_1	537.95	000	A_1	466.61
100	A_2	115.25	111	A_2	560.26		A_2	466.61
010	A_2	206.55	030	A_2	581.08	100	A_1	557.64
200	A_1	226.19	301	A_1	585.09		A_2	557.64
001	A_2	255.24	102	A_2	610.44	200	A_1	655.35
110	A_1	321.21	600	A_1	621.11		A_2	655.35
300	A_2	332.63	220	A_1	623.96	010	A_1	659.09
101	A_1	369.26	021	A_2	630.09		A_2	659.09
020	A_1	401.77	410	A_2	639.12	001	A_1	710.45
210	A_2	431.70	211	A_1	669.88		A_2	710.45
400	A_1	434.26	012	A_2	669.95	300	A_1	746.77
011	A_1	446.15	130	A_1	682.01		A_2	746.77
201	A_2	479.31	401	A_2	686.19	110	A_1	755.96
002	A_1	497.56	700	A_2	704.94		A_2	755.96
120	A_2	515.14	202	A_1	719.38	101	A_1	800.15
500	A_2	530.65					A''	800.15

[a]ZPVE=315.639 cm^{-1}.

Table III displays the displacements of the torsional levels by Fermi resonances involving medium amplitude vibrations calculated with PT2 algorithm implemented in GAUSSIAN 03.[21] The effects of the vibrational resonances are only noticeable for the $(vv'v'')=(110)$ torsional level and few combination bands involving torsion and other low frequency modes (CH_3 rock and COC bending). The few and small significant displacements assure that torsional modes may be treated independent of the remaining vibrations. Furthermore, the x_{ij} $(i<28; j>27)$ anharmonic constants can be also employed to test the validity of the reduced 3D model and the coordinate independence. For *trans*-EME, few interaction constants are significant: $x_{2917}=5.743$ and $x_{2827}=5.453$ (in cm^{-1}); for the *cis-gauche*-EME, the largest ones are $x_{2230}=3.760$, $x_{2629}=-4$, $x_{2628}=-4.128$, and $x_{2729}=5.566$ (in cm^{-1}).

The determination of a fourth-order anharmonic force field for a molecule with 12 atoms, as is EME, represents a large computational effort. For this reason, we provide in Table IV the harmonic MP2, anharmonic MP2, and harmonic CCSD fundamentals for the $3n-9$ vibrations. For their relevance to this paper, the torsional band positions are presented in Table V, where we compare them with the variational calculations described in further sections. All the results are compared with the experimental data from Durig *et al.*,[14] observing a good correlation between experiments and calculations.

C. The FIR spectrum

Torsional energy levels were calculated variationally by solving a pure torsional Hamiltonian depending on three coordinates. Thus,

$$\hat{H}(\alpha,\theta_1,\theta_2) = -\sum_{i=1}^{3}\sum_{j=1}^{3}\left(\frac{\partial}{\partial q_i}\right)B_{q_iq_j}(\alpha,\theta_1,\theta_2)\left(\frac{\partial}{\partial q_j}\right) + V(\alpha,\theta_1,\theta_2) + V^{I}(\alpha,\theta_1,\theta_2) + V^{\mathrm{ZPVE}}(\alpha,\theta_1,\theta_2),$$

$$q_i,q_j=\alpha,\theta_1,\theta_2. \quad (2)$$

Here, B_{ij} represents the G kinetic energy matrix vibrational elements expressed in cm^{-1}; V, V', and V^{ZPVE} are the 3D-PES, the Podolsky pseudopotential, and the ZPVE, respectively. All the parameters transform as the totally symmetric representation of the G_{18} nonrigid group.[25]

The 3D-PES has been computed from the CCSD(T)/cc-pVTZ energies of a grid of 181 selected geometries determined by optimizing $3n-9$ at the CCSD/cc-pVTZ level of theory. The kinetic energy parameters and the ZPVE have been calculated for each structure and fitted to a triple Fourier series formally identical to Eq. (1). The expansion coefficients for the parameters are published as supplementary material.[26] The ZPVE correction allows to one consider vibrational effects derived from the interactions with the neglected $3n-9$ coordinates, which are partially taken into consideration during the geometry optimization. For saving computational expenses, ZPVE has been determined with MP2/cc-pVTZ because very small advantage may be expected from CCSD theory.

An original set of 148 geometries has been selected for specific values of the three C4C2CO1C3, H7C3O1C2, and H10C4C2O1 dihedral angles, comprised of 180° and 0°. For C4C2O1C3, which defines the ethyl torsion, the grid interval was 20°. For the methyl coordinates, we choose four values (180°, 90°, −90°, and 0°), in which one of the hydrogens is forced to lie in the molecular plane or perpendicular to it, following the recommendation of Smeyers and Villa[27] to

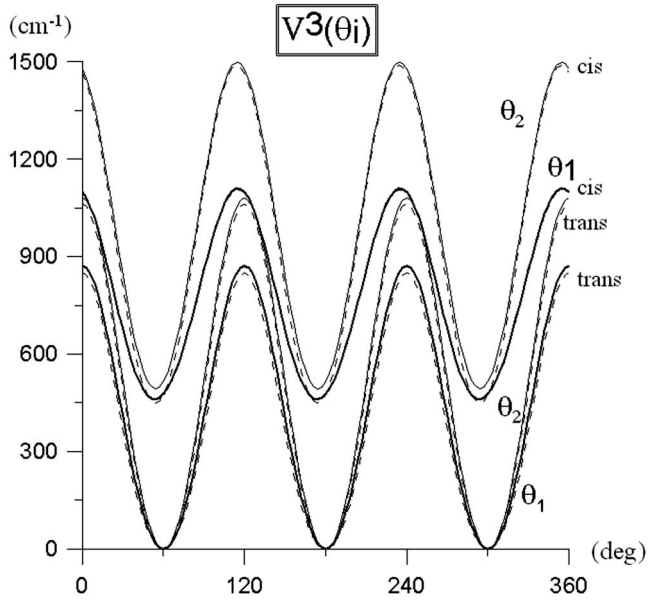

FIG. 3. One-dimensional cuts of the PES for *trans*- and *cis-gauche*-ethyl methyl ether along the methyl torsional coordinates, θ_1 and θ_2.

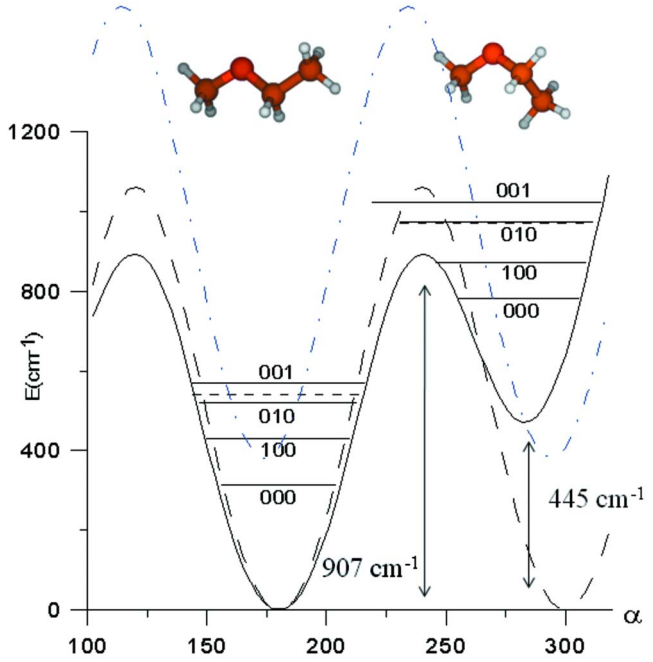

FIG. 4. (Color online) The fundamental energy levels corresponding to the three torsional modes of *trans* and *cis-gauche*-ethyl methyl ether.

avoid what they call the "*symmetry dilemma*." In Ref. 27, one hydrogen dihedral angle is identified to the vibrational coordinate (θ_1=H7C3O1C2 and θ_2=H10C4C2O1, for EME).

Many solutions have been proposed to search for a correct definition of methyl torsional coordinates and to correct the subsequent numerical inaccuracy.[27–30] In a complex molecule as EME, methyl groups present slightly distorted C_{3v} structures, whereas the "*dynamical* C_{3v} symmetry" is preserved during the torsional motion generating the PES threefold periodicity. If this problem is not well treated, an artificial symmetry break is added during the 3D-PES calculation because one dihedral angle corresponding one to of the methyl hydrogen atom should be frozen (H7C3O1C2 or H10C4C2O1), whereas the remaining hydrogen dihedral angles are allowed to be relaxed to complete a set of $3n-9$ optimized coordinates. The different ways of treating the methyl hydrogen introduce a numerical error minimizable for planar molecules with the well fundamental geometry selection of Smeyers and Villa,[27] the coordinate definition of which produces slightly low energies and fails for nonplanar structures.

Recently,[30] we have completed a rigorous new study of the problem. Symmetry criteria have been applied to obtain a correct definition of the torsional coordinate. Thus, for example, for the first methyl group, the three angles, γ_1 =H7C3O1C2, γ_2=H8C3O1C2, and γ_3=H9C3O1C2 are used to perform linear combinations of internal coordinates and to define the torsional coordinate θ_1 and two deformation coordinates α_1 and α_2,

$$\theta_1 = (\gamma_1 + \gamma_2 + \gamma_3 - 2\pi)/3, \quad \alpha_1 = (\gamma_2 - \gamma_3)/2,$$

$$\beta_1 = \gamma_1/2 - (\gamma_2 + \gamma_3)/4.$$

The application of this definition, which has a clear physical meaning, presents serious practical problems given the lack of available optimization methods for high level of *ab initio* theory when linear combinations of internal coordinates are used. For our 3D problem, one of the coordinates θ_1 should be frozen, whereas the two deformation coordinates, α_1 and β_1, should be optimized. To avoid this practical limitation, we add new geometries to the first selected following the recommendation of Ref. 23 (for example, for γ_1 $=30°, 60°, 120°, 150°, \ldots$). These additional geometries lie close to the minimum energy structures and complete a set of 181 structures. Energies and geometries are fitted to an analytic function as in Eq. (1) after adding terms for the deformation coordinates that are minimized. This correction is called *DihC* in this paper.

The Hamiltonian was solved variationally using symmetry eigenvectors corresponding to the G_{18} nonrigid group as trial functions (see Table I, in Ref. 25). An acceptable numerical convergence requires $119\,474 = 59 \times 45 \times 45$ basis functions. The symmetry conditions factorize the Hamiltonian matrix into boxes that have dimensions of 6638 (A_1 and A_2) and 13 275 (E_1, E_2, E_3, E_4). Table V displays the fundamental frequencies for each mode, whereas Table VI shows the *trans* and *cis-gauche* levels for the nondegenerate symmetry species A_1 and A_2 up to 700 cm^{-1} (*trans*) and 800 cm^{-1} (*cis-gauche*). In Fig. 4, the first energy levels are localized in the minima. Each 3D level i is localized in the *trans* and *cis-gauche* minima using the probability integral,

$$\int_{\alpha_{\min}-x}^{\alpha_{\min}+x} \varphi_i^* \varphi_i d\alpha \tag{3}$$

and classified using the vibrational quanta ($vv'v''$). For this last purpose, we determine integrals for one-dimensional terms of the Hamiltonian in Eq. (2),

TABLE VII. Band positions (in cm^{-1}) and intensities corresponding to the three torsional modes of *trans*-ethyl methyl ether, calculated at the CCSD(T) level.

Assign.	Symmetry	ν	Intensity (273 K)	Expt. (Ref. 14) ν (intensity)	Assign.	Symmetry	ν	Intensity (273 K)	Expt. (Ref. 14) ν (intensity)
				Skeletal torsion					
$000\rightarrow100$	$A_1\rightarrow A_2$	115.3	0.41×10^{-4}	115.40 (vs)	$300\rightarrow400$	$A_2\rightarrow A_1$	101.6	0.34×10^{-4}	103.54
	$E_1\rightarrow E_1$	115.3	0.81×10^{-4}			$E_1\rightarrow E_1$	101.6	0.68×10^{-4}	
	$E_2\rightarrow E_2$	115.3	0.81×10^{-4}			$E_2\rightarrow E_2$	101.7	0.68×10^{-4}	
	$E_3\rightarrow E_3$	115.3	0.41×10^{-4}			$E_3\rightarrow E_3$	102.1	0.34×10^{-4}	
	$E_4\rightarrow E_4$	115.3	0.41×10^{-4}			$E_4\rightarrow E_4$	102.1	0.34×10^{-4}	
$100\rightarrow200$	$A_2\rightarrow A_1$	110.9	0.48×10^{-4}	111.77	$400\rightarrow500$	$A_1\rightarrow A_2$	96.4	0.27×10^{-4}	99.0
	$E_1\rightarrow E_1$	111.1	0.96×10^{-4}			$E_1\rightarrow E_1$	96.4	0.34×10^{-4}	
	$E_2\rightarrow E_2$	111.1	0.96×10^{-4}			$E_2\rightarrow E_2$	96.4	0.34×10^{-4}	
	$E_3\rightarrow E_3$	111.1	0.48×10^{-4}			$E_3\rightarrow E_3$	96.4	0.27×10^{-4}	
	$E_4\rightarrow E_4$	111.1	0.48×10^{-4}			$E_4\rightarrow E_4$	96.4	0.27×10^{-4}	
$200\rightarrow300$	$A_1\rightarrow A_2$	106.4	0.42×10^{-4}	107.80					
	$E_1\rightarrow E_1$	106.4	0.84×10^{-4}						
	$E_2\rightarrow E_2$	106.5	0.84×10^{-4}						
	$E_3\rightarrow E_3$	106.1	0.42×10^{-4}						
	$E_4\rightarrow E_4$	106.1	0.42×10^{-4}						
				Methyl torsions					
$000\rightarrow010$	$A_1\rightarrow A_2$	206.6	0.31×10^{-4}	202 (m)	$000\rightarrow001$	$A_1\rightarrow A_2$	255.2	0.24×10^{-5}	248 (m)
	$E_1\rightarrow E_1$	206.6	0.61×10^{-4}			$E_1\rightarrow E_1$	255.2	0.47×10^{-5}	
	$E_2\rightarrow E_2$	206.6	0.61×10^{-4}			$E_2\rightarrow E_2$	255.2	0.47×10^{-5}	
	$E_3\rightarrow E_3$	206.6	0.31×10^{-4}			$E_3\rightarrow E_3$	255.2	0.24×10^{-5}	
	$E_4\rightarrow E_4$	206.6	0.31×10^{-4}			$E_4\rightarrow E_4$	255.2	0.24×10^{-5}	
$010\rightarrow020$	$A_2\rightarrow A_1$	195.2	0.19×10^{-4}		$001\rightarrow002$	$A_2\rightarrow A_1$	242.3	0.19×10^{-5}	
	$E_1\rightarrow E_1$	195.2	0.19×10^{-4}			$E_1\rightarrow E_1$	242.3	0.38×10^{-5}	
	$E_2\rightarrow E_2$	195.5	0.38×10^{-4}			$E_2\rightarrow E_2$	242.3	0.38×10^{-5}	
	$E_3\rightarrow E_3$	195.5	0.38×10^{-4}			$E_3\rightarrow E_3$	242.3	0.19×10^{-5}	
	$E_4\rightarrow E_4$	195.5	0.19×10^{-4}			$E_4\rightarrow E_4$	242.3	0.19×10^{-5}	
$020\rightarrow030$	$A_1\rightarrow A_2$	179.3	0.90×10^{-5}		$002\rightarrow003$	$A_1\rightarrow A_2$	230.0	$<10^{-5}$	
	$E_1\rightarrow E_1$	179.3	0.18×10^{-4}			$E_1\rightarrow E_1$	230.0	$<10^{-5}$	
	$E_2\rightarrow E_2$	179.4	0.18×10^{-4}			$E_2\rightarrow E_2$	230.1	$<10^{-5}$	
	$E_3\rightarrow E_3$	179.4	0.90×10^{-5}			$E_3\rightarrow E_3$	230.1	$<10^{-5}$	
	$E_4\rightarrow E_4$	179.4	0.90×10^{-5}			$E_4\rightarrow E_4$	230.1	$<10^{-5}$	
				Combination bands					
$100\rightarrow110$	$A_2\rightarrow A_1$	206.0	0.15×10^{-4}		$210\rightarrow310$	$A_2\rightarrow A_1$	106.1	0.15×10^{-4}	
$010\rightarrow110$	$A_2\rightarrow A_1$	114.7	0.14×10^{-4}		$101\rightarrow201$	$A_1\rightarrow A_2$	110.1	0.15×10^{-4}	
$001\rightarrow101$	$A_2\rightarrow A_1$	114.0	0.11×10^{-4}		$201\rightarrow301$	$A_2\rightarrow A_1$	105.8	0.11×10^{-4}	
$110\rightarrow210$	$A_1\rightarrow A_2$	116.0	0.16×10^{-4}		$001\rightarrow011$	$A_2\rightarrow A_1$	190.9	0.65×10^{-5}	

$$\langle \hat{H}_q \rangle = \langle \varphi_i | - B_q^0 \frac{\partial^2}{\partial q^2} + V(q) | \varphi_i \rangle, \quad q = \alpha, \theta_1, \theta_2. \tag{4}$$

For the lowest levels, the tunneling splitting is very small (<0.1 cm^{-1}). It is necessary to go above 700 cm^{-1} to obtain significant gaps, where transitions are really weak at 273 K. Splittings larger than 0.1 cm^{-1} are expected for bands connecting excited states above (0,3,0) or (0,0,3). For the ethyl torsional modes, A_1 and A_2 levels over (7,0,0) are degenerate. For the *gauche*-form, fundamental transition splittings are also lower than 0.1 cm^{-1}.

Table V summarizes the fundamental frequencies calculated with MP2 and CCSD. CCSD and MP2 harmonic and MP2 anharmonic frequencies are determined with the corresponding algorithms implemented in the Gaussian. CCSD(T) and MP2 anharmonic ones are obtained by solving variationally a 3D Hamiltonian. Variational results are shown in three different columns: the two first column results (3D and 3D +ZPVE) have been performed with the definition of Ref. 27 for the methyl coordinates, whereas the third column results (3D+ZPVE+DihC) have been achieved using the *DihC method* described above.

MP2 calculations allow one to compare PT2 and variational energies. It may be emphasized how the variational results for the *trans*-form (261.4, 211.3, and 118.1 cm^{-1}) are in very good agreement with the PT2 anharmonic frequencies (259, 211, and 118 cm^{-1}), which proves that the *DihC* correction is adequate for the correct coordinate definition. In the case of the *cis-gauche*-form, the ν_{28} fundamental seems to be an exception ($\nu_{28}=250.9$ cm^{-1} with 3D+ZPVE +DihC, $\nu_{28}=242$ cm^{-1} with PT2), but, as it lies over the *trans*$\rightarrow$*cis-gauche* barrier (see Fig. 4), the PT2 theory is responsible for the error since it fails in describing the interactions between both conformer levels. The evolution of

TABLE VIII. Fundamental band positions (the fundamental transitions splittings are lower than 0.1 cm^{-1}) (in cm^{-1}) and intensities corresponding to the three torsional modes of *cis-gauche*-ethyl methyl ether, calculated at the CCSD(T) level of theory.

Assign.	Symmetry	Band position	Intensity (273 K)	Expt. (Ref. 14) ν (intensity)
$0^+00 \rightarrow 1^-00$	$A_1 \rightarrow A_2$	91.0	0.62×10^{-6}	93.56 (m)
$0^-00 \rightarrow 1^+00$	$A_2 \rightarrow A_1$	91.0	0.62×10^{-6}	93.56 (m)
$0^+00 \rightarrow 0^-10$	$A_1 \rightarrow A_2$	192.5	0.82×10^{-7}	
$0^-10 \rightarrow 0^+10$	$A_2 \rightarrow A_1$	192.5	0.82×10^{-7}	
$0^+00 \rightarrow 0^-01$	$A_1 \rightarrow A_2$	243.8	0.29×10^{-7}	
$0^-10 \rightarrow 0^+01$	$A_2 \rightarrow A_1$	243.8	0.29×10^{-7}	

CCSD results with the corrections is very similar to the MP2 one.

ZPVE is the most important correction in models depending on the number of coordinates less than $3n-6$.[24,30] In EME, this is really evident for ν_{30}, which is independent of the DihC correction defined for the CH_3 internal rotation. For the skeletal torsion, the CCSD(T) variational calculations, 115.3 cm^{-1} (*trans*) and 91.0 cm^{-1} (*cis-gauche*), are in very good agreement with the measurements (115.4 and 94 cm^{-1}).[14] For methyl groups, the definition of coordinates in Ref. 25 produces slightly low frequencies, whereas the DihC correction gives slightly high values. Both methods are real solution borders which allow confinement of the center band between 196.6 and 206.6 cm^{-1} and 146 cm^{-1} and 255.2 cm^{-1}. For the *cis-gauche*-form, the two bands for CH_3 torsion are centered at 192.5 and 243.8 cm^{-1}. Calculated frequencies and intensities force us to search for a new assignment for the gas phase FIR spectrum of Durig *et al.*[14]

Table V shows also the *trans* fundamental frequencies for the $CD_3-O-CH_2-CH_3$ isotopomer. In this case, our calculations confirm the assignments of Durig *et al.*[14] Differences between calculations and observations are of the same order of magnitude for both isotopomers only if the new assignment for the hydrogenated species is taken into consideration. The *EME-d*$_3$ results confirm our new assignment for $CH_3-O-CH_2-CH_3$.[31]

Intensities have been computed at room temperature (see Tables VII and VIII) to simulate laboratory conditions, and at 10 K, to simulate interstellar environments. We employed the oscillator strength equation:[32]

$$I = \frac{Wq}{R^2 e^2 \bar{B}}(E_j - E_i)(P_j - P_i)\langle\varphi_j|\mu|\varphi_i\rangle^2. \quad (5)$$

Here, E_j-E_i represents the transition frequency and P_j and P_i are Boltzmann populations; Wq is the nuclear statistical weight multiplied by the vibrational degeneration (see G_{18} character table in Ref. 25); e, R, and $\bar{B}$ are the electron charge, the averaged internal rotation radius, and the kinetic energy parameter average, respectively, which are calculated using the equilibrium geometries since their change is unnoticeable in the intensities for transitions between low energy levels; μ is the dipole moment, which was calculated for each conformation at the MP2/cc-pVTZ level and later on fitted to an adapted symmetry Fourier series. For a near prolate as is EME, only type *A* and type *C* bands present prominent *Q* branches. In addition, for the out-of-plane torsional modes, only the μ_C component is responsible for strong bands.

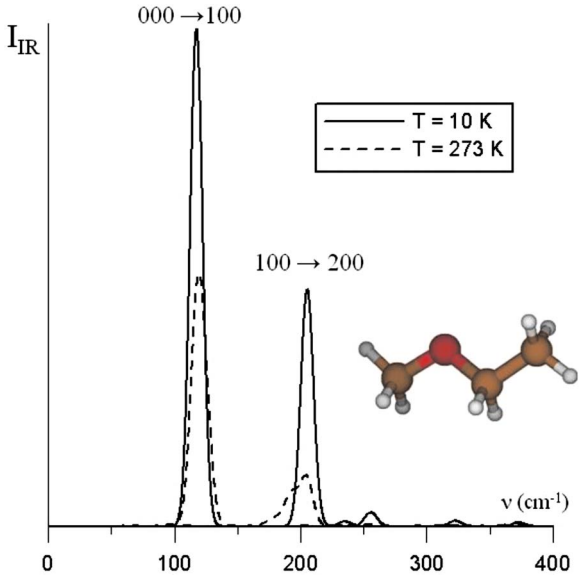

FIG. 5. (Color online) The FIR spectrum of ethyl methyl ether calculated at 273 and 10 K.

In Fig. 5, the FIR spectra at 273 K (dashed line) and 10 K (solid line) are compared. Strongest bands correspond to ν_{30} mode excitations, which carry out the most significant dipole moment variation. At 10 K, the single prominent bands are for the fundamental transitions. The differences in intensities between tunneling components arise from the nuclear statistical weights and the vibrational degeneration. E_1 and E_2 components show the largest intensities.

At 273 K, the transitions corresponding to the *cis-gauche* conformer are very weak as a consequence of the Boltzmann population. For this reason, we believe that the medium intensity band observed at 202 cm^{-1} needs to be reassigned to the *trans*-form (ν_{29} mode). Previous assignments, based on the MP2/6-31G** harmonic calculations, need to be revised on the base of our new anharmonic frequencies performed at high level of theory [CCSD(T)/cc-pVTZ].

Finally, in Table IX, rotational constants and the asymmetrically reduced Hamiltonian parameters calculated with MP2 (PT2) are shown. Expectation values of the CCSD rotational constants are also determined for the 3D-PES. Theoretical predictions are compared with the ground vibrational state parameters of Fuchs *et al.*[3] and first excited vibrational state rotational constants of Kobayashi *et al.*[7]

IV. CONCLUSIONS

In this paper, frequencies and intensities of the FIR spectrum of EME are predicted from a CCSD(T)/cc-pVTZ PES. The vibrational ZPVE correction of the PES and a careful definition of the coordinates allow one to obtain accurate variational energy levels.

By taking frequencies and intensities into consideration, a new assignment of previous experimental bands, congruent

TABLE IX. MP2 rotational parameters (in MHz) calculated with second order perturbation theory. Rotational constant expectation values (in MHz) calculated from the CCSD(T) 3D-PES.

	trans-EME			*cis-gauche*-EME	
	MP2 (PT2)	CCSD(T) $\langle\varphi^*\|ABC\|\varphi\rangle$	Expt.	MP2 (PT2)	CCSD(T) $\langle\varphi^*\|ABC\|\varphi\rangle$
A_{000}	27 280.341	28 115.91	27 991.7139[a]	15 898.466	16 089.00
B_{000}	4184.750	4189.39	4159.443 14[a]	5165.583	5214.56
C_{000}	3890.793	3922.50	3891.136 34[a]	4503.450	4555.11
A_{100}	26 826.693	27 836.42	27 527.7046[b]	16 185.17	16 226.64
B_{100}	4185.01	4191.62	4160.106 55[b]	5104.66	5199.01
C_{100}	3899.58	3932.67	3899.963 88[b]	4496.26	4550.65
A_{200}	26 372.72	27545.06		16 471.47	16 418.23
B_{200}	4185.51	4194.28		5043.16	5161.88
C_{200}	3908.31	3942.98		4488.96	4538.90
A_{300}	25 919.13	27238.99		16 758.07	16 371.90
B_{300}	4185.81	4197.28		4982.00	5162.27
C_{300}	3917.00	3954.19		4481.79	4536.37
A_{010}	27 110.53	28129.16		15 849.64	16 108.42
B_{010}	4179.41	4186.97		5173.70	5216.49
C_{010}	3899.58	3920.59		4501.44	4550.49
A_{001}	27 150.94	28114.14		16 229.41	16 272.64
B_{001}	4179.62	4186.04		5065.50	5163.66
C_{001}	3887.29	3919.26		4470.15	4537.30
	Vibrational ground state spectroscopic parameters				
Δ_J	$0.530\,908\times10^{-3}$			$0.784\,333\times10^{-2}$	
Δ_K	0.557 117			0.181 102	
Δ_{JK}	0.061 570			−0.047 658	
δ_j	$-0.130\,995\times10^{-3}$			$0.283\,114\times10^{-2}$	
δ_k	0.012 300			0.028 549	
κ	−0.977 348 62			−0.873 665	

[a]Reference 3.
[b]Reference 7.

with the new *ab initio* results, is proposed. For the most stable *trans*-conformer, the ν_{30}, ν_{29}, and ν_{28} fundamentals, computed at 115.3, 206.5, and 255.2 cm^{-1}, are correlated with the observed bands at 115.4, 202, and 248 cm^{-1}. For the *cis-gauche* the three band positions are computed at 91.0, 192.5, and 243.8 cm^{-1}.

The tunneling splittings of the levels are not distinguishable below 700 cm^{-1}, where IR bands are really weak at 273 K. Splittings larger than 0.1 cm^{-1} are expected for bands connecting excited states above (0,2,0) or (0,0,3).

ACKNOWLEDGMENTS

This work has also been supported by the Ministerio de Educación of Spain, Grant No. AYA2005-00702 [Plan Nacional I+D+I (2004–2007)], CONACYT of Mexico, Grant No. 58728 CoNaCYT, and Computing resources of CESGA. M.L.S. wants to acknowledge Professor J. T. Hougen for help and useful comments.

[1] G.W. Fuchs, U. Fuchs, T. F. Giesen, and F. Wyrowski, Astron. Astrophys. **444**, 521 (2005).
[2] S. B. Charnley, M. E. Kress, A. G. G. M. Tielens, and T. J. Millar, Astrophys. J. **448**, 232 (1995).
[3] U. Fuchs, G. Winnewisser, P. Groner, F. C. de Lucia, and E. Herbst, Astrophys. J. **144**, 277 (2003).
[4] M. Hayashi and K. Kuwada, J. Mol. Struct. **28**, 147 (1975).
[5] M. Hayashi and M. Adachi, J. Mol. Struct. **78**, 53 (1982).
[6] S. Tsunekawa, Y. Kinai, Y. Kondo, H. Odashima, and K. Takagi, Molecules **8**, 103 (2003).
[7] K. Kobayashi, T. Matsui, N. Mori, S. Tsunekawa, and N. Ohasshi, J. Mol. Spectrosc. **251**, 301 (2008).
[8] Y. Shiki, N. Ibushi, M. Oyamada, J. Nakagawa, and M. Hayashi, J. Mol. Spectrosc. **87**, 357 (1981).
[9] J. R. Durig and D. J. Gerson, J. Mol. Struct. **71**, 131 (1981).
[10] J. Nakagawa, M. Imachi, and M. Hayashi, J. Mol. Struct. **112**, 201 (1984).
[11] M. Fujitake and M. Hayashi, J. Mol. Struct. **127**, 21 (1985).
[12] A. Suwa, H. Ohta, and S. Konaka, J. Mol. Struct. **172**, 275 (1988).
[13] I. Medvedev, M. Winnewisser, F. C. de Lucia, E. Herbst, E. Yi, L. P. Leong, R. P. A. Bettens, E. Bialkowska-Jaworska, O. Desyatnyk, L. Pszczólkowski, and Z. Kisiel, Astrophys. J., Suppl. Ser. **148**, 593 (2003).
[14] J. R. Durig, Y. Jin, H. V. Phan, and D. T. Durig, Struct. Chem. **13**, 1 (2002).
[15] G. E. Scuseria and H. F. Schaefer III, J. Chem. Phys. **90**, 3700 (1989); J. A. Pople, M. Head-Gordon, and K. Raghavachari, *ibid.* **87**, 5968 (1987).
[16] M. L. Senent, D. C. Moule, and Y. G. Smeyers, J. Chem. Phys. **102**, 5952 (1995).
[17] M. L. Senent, Y. G. Smeyers, R. Dominguez-Gómez, and M. Villa, J. Chem. Phys. **112**, 5809 (2000).
[18] M. L. Senent, M. Villa, F. J. Meléndez, and R. Domínguez-Gómez, Astrophys. J. **627**, 567 (2005).
[19] P. Groner, J. Chem. Phys. **107**, 4483 (1997).
[20] W. H. Miller, R. Hernandez, N. C. Handy, D. Jayatilaka, and A. Willets, Chem. Phys. Lett. **172**, 62 (1990).
[21] M. J. Frisch, G. W. Trucks, H. B. Schlegel *et al.*, GAUSSIAN 03, Revision C.02, Gaussian, Inc., Wallingford, CT, 2004.
[22] M. L. Senent, ENEDIM (http://damir.iem.csic.es/~senent/PROGRAMAS.htm).
[23] M. L. Senent, Mol. Phys. **99**, 1311 (2001).

[24] A. G. Császár, V. Szalay, and M. L. Senent, J. Chem. Phys. **120**, 1203 (2004).
[25] N. Ohashi, J. T. Hougen, R. D. Suenram, F. J. Lovas, Y. Kawashima, M. Fujitake, and J. Pyka, J. Mol. Spectrosc. **227**, 28 (2004).
[26] See EPAPS Document No. E-JCPSA6-130-011906 for potential energy surface coefficients. For more information on EPAPS, see http://www.aip.org/pubservs/epaps.html.
[27] Y. G. Smeyers and M. Villa, Chem. Phys. Lett. **235**, 587 (1995).
[28] L. Goodman, J. Leszczynski, and T. Kundu, J. Chem. Phys. **100**, 1274 (1994).
[29] C. Muñóz-Caro, A. Niño, and D. C. Moule, J. Mol. Struct. **350**, 83 (1995).
[30] V. Szalay, A. G. Csàszár, and M. L. Senent, J. Chem. Phys. **117**, 6489 (2002).
[31] M. Villa, M. L. Senent, and R. Dominguez-Gómez, Chem. Phys. Lett. **436**, 15 (2007).
[32] Y. G. Smeyers, M. L. Senent, V. Botella, and D. C. Moule, J. Chem. Phys. **98**, 2754 (1993).